Crossover behavior in micellar solutions with lower critical demixing point: Broadband ultrasonic spectrometry of the isobutoxyethanol-water system

K. Menzel,[1] S. Z. Mirzaev,[1,2] and U. Kaatze[1,*]
[1]*Drittes Physikalisches Institut, Georg-August-Universität, Bürgerstrasse 42-44, 37073 Göttingen, Germany*
[2]*Heat Physics Department, Uzbekistan Academy of Sciences, Katartal 28, Tashkent 700132, Uzbekistan*
(Received 31 January 2003; published 9 July 2003)

The aggregation kinetics of isobutoxyethanol-water mixtures with lower critical demixing point has been investigated. Two types of kinetics have been observed, a diffusion-controlled formation of micellar species and the formation of a microheterogeneous liquid structure, governed by fluctuations in the local concentration. Ultrasonic attenuation spectra of isobutoxyethanol-water mixtures have been measured between 100 kHz and 2 GHz at 25 °C and at several concentrations, covering the complete composition range. With the mixture of critical composition measurements have been performed at some temperatures near the critical temperature ($T_c = 299.51$ K). In addition to the asymptotic high frequency background contribution, the broadband spectra reveal a Bhattacharjee-Ferrell relaxation term due to critical concentration fluctuations, a restricted Hill term reflecting the monomer exchange between micelles and the suspending phase, and two Debye-type relaxation terms that are assigned to chemical relaxations. The relaxation rates of the Bhattacharjee-Ferrell term exceed those from static and dynamic light scattering (amplitude $\Gamma_0 = 5.3 \times 10^9$ s^{-1}), likely due to the effect of a second parallel pathway of relaxation in the ultrasonic field. The adiabatic coupling constant following from the amplitude in the ultrasonic spectrum agrees with that from a thermodynamic relation ($g = 1.3$). The restricted Hill term displays the features of an extended Teubner-Kahlweit-Aniansson-Wall model of the micelle formation and decay kinetics in surfactant solutions with high critical micelle concentration ($C = 0.6$ mol/ℓ). The idea of a fluctuation controlled monomer exchange in aqueous solutions of poly(ethylene glycol) monoalkyl ether-water mixtures near the critical point is briefly discussed.

DOI: 10.1103/PhysRevE.68.011501 PACS number(s): 83.80.Qr

I. INTRODUCTION

The structure and microdynamics of liquid mixtures are controlled by a delicate interplay of solvophilic and solvophobic interactions. A prominent example in biophysics is the formation of bilayer membranes from lipid molecules in water [1]. In order to effectively reduce contact of hydrophobic parts of membrane molecules with water, the chains of the lipids form a nonpolar phase, separated from the solvent by polar head groups. Depending on their shape other amphiphilic molecules, when dissolved in water, can achieve segregation of their hydrophobic parts also by forming spherically, ellipsoidally, or cylindrically shaped micelles. The nonpolar parts of the amphiphiles are then squeezed in the core of the multimolecular structure. The free energy of a binary liquid may be also minimized by separation into two phases, differing from one another by the concentration of the constituents. Much attention has been directed toward critically demixing binary liquids [2–7], because concentration fluctuations over a vast range of sizes exist near the critical demixing point. These fluctuations mask specific properties and thus lead to universal characteristics of systems which show otherwise strikingly different behavior. Despite of the wide interest in critically demixing liquids, at present it is not generally clear which features of the molecular interactions are important in propagating the interparticle correlations throughout a macroscopic system and which are unimportant for the overall critical behavior but determine the individual properties of the system.

The opinion is commonly held that a binary liquid minimizes its free energy by undergoing only one critical phenomenon, formation of micellar structures or demixing. However, recent ultrasonic studies of mixtures of water with various poly(ethylene glycol) monoalkyl ethers (C_iE_j) indicated micelles and fluctuations in the concentration to exist simultaneously [8]. These indications have prompted us to perform a broadband ultrasonic spectrometry study of mixtures of water with 2-isobutoxyethanol (i-C_4E_1). So far, conflicting aspects of this binary system have been reported. Light scattering [9] and heat capacity data [10] clearly exhibited critical behavior. Ultrasonic spectra for the i-C_4E_1–H_2O system, however, have been alternatively discussed. Fanning and Kruus assigned their excess attenuation data to structure relaxation processes but mentioned, in addition, indications of some low frequency contributions from critical phenomena [11]. Later, Nikishawa and co-workers discussed their spectra in terms of two well-defined chemical equilibria, one reflecting the formation of solute-solute and the other one solute-solvent complexes [12,13]. Recently, the concentration dependence in the maximum amplitude of the ultrasonic attenuation of mixtures of water with longer C_iE_j has been extrapolated to predict a critical micelle concentration of the order of 0.6 mol/ℓ for the i-C_4E_1–H_2O system (Fig. 1). Even though micelle formation of short amphiphilic molecules may not result in well-defined proper aggregates with narrow size distribution, as is the case with long-chain amphiphiles in water, the simultaneous presence of two criti-

*Electronic address: uka@physik3.gwdg.de

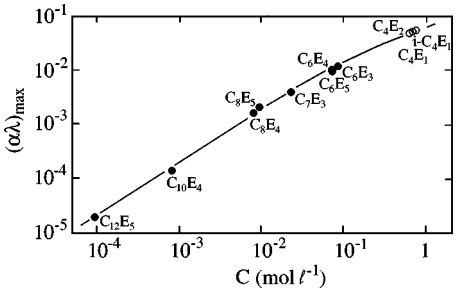

FIG. 1. Maximum values $(\alpha\lambda)_{max}$ in the ultrasonic excess attenuation spectra $(\alpha\lambda)_{exc}=\alpha\lambda-B\nu$ of mixtures of poly(ethylene glycol) monoalkyl ethers $[CH_3(CH_2)_{i-1}(OCH_2CH_2)_jOH,C_iE_j]$ with water displayed as a function of the critical micelle concentration C [8]. Full symbols indicate systems with well defined C.

cal phenomena opens fascinating aspects. Particularly interesting is the question whether or not constraints in the extent of concentration fluctuations exist and whether the diameter of the micelles, as a second characteristic length, possess special effects in the power law behavior and kinetics of the critical system.

II. MATERIALS

A. 2-Isobutoxyethanol solutions

2-Isobutoxyethanol (i-C_4E_1, purity $\geqslant$97%) was purchased from Wako (Japan). The original material has been purified using two different methods. First, the three-phase extraction technique [14,15] has been applied. For this purpose, 150 ml of a saturated mixture of *n*-propanol (Fluka, Germany, $\geqslant$99.5%) and quartz bidistilled water were added to 100 g i-C_4E_1 and 120 ml *n*-octane (Fluka, $\geqslant$99.5%) to follow the procedure described in the literature [14,15]. The phase separation curve was measured for i-C_4E_1–H_2O mixtures with compositions near the critical composition. A lower critical temperature $T_c=299.67$ K was found which is somewhat superior to the literature value $T_c=299.61$ K [16]. As the yield from the three-phase extraction procedure is 20% only, we additionally purified the initial i-C_4E_1 material by fractional distillation at 318 K and reduced pressure (23 mbar) in a concentric tube column of 64 real plates. The critical temperature reached with such distilled i-C_4E_1 was $T_c=299.51$ K at a mass fraction $Y=0.330$ of surfactant. The slightly lower T_c is assumed to be due to small traces of water that may still be present after the fractional distillation of the isobutoxyethanol.

Mixtures of different i-C_4E_1 concentration were prepared by weighing appropriate amounts of the constituents into suitable flasks. A survey of the mixtures is presented in Table I, where besides the concentration data the density ρ and the shear viscosity η_s at 25 °C as well as the phase separation temperature T_p are also given. The density has been measured pycnometrically, the shear viscosity has been determined with a falling ball viscosimeter (type B/BH, Haake, Karlsruhe, Germany).

TABLE I. Mole fraction X, mass fraction Y, and concentration c of surfactant as well as density ρ, shear viscosity η_s at 25 °C, and phase separation temperature T_p of the i-C_4E_1–water mixtures.

X ±0.2%	Y ±0.1%	c (mol ℓ^{-1}) ±0.2%	ρ (g cm^{-3}) ±0.1%	η_s (mPa s) ±0.2%	T_p (K)
0.011	0.070	0.587	0.9947	1.119	
0.015	0.090	0.759	0.9937	1.194	316.85
0.020	0.120	1.009	0.9918	1.320	309.95
0.026	0.150	1.256	0.9894	1.500	303.71
0.041	0.220	1.828	0.9822	1.961	299.91
0.061	0.300	2.472	0.9738	2.550	299.47
0.070	0.330	2.711	0.9710	2.748	299.51
0.099	0.420	3.418	0.9620	3.164	300.55
0.168	0.570	4,561	0.9456	3.646	307.28
0.262	0.700	5.513	0.9307	3.920	343.15
0.379	0.800	6.219	0.9185	3.891	
1.000	1.000	7.531	0.8900		

B. Acoustical attenuation spectrometry

Between 100 kHz and 2 GHz the acoustical attenuation coefficient α of the liquids has been measured as a function of frequency ν using two methods. At low frequencies ($\nu<15$ MHz), where α is small, a resonator technique has been applied in which the path length of interaction of the sonic wave and the sample is virtually increased by multiple reflections. The liquid was contained in a circular cavity, the end faces of which were formed by planar transducer discs made of piezoelectric quartz. The attenuation coefficient was actually measured from the change in the quality factor of resonance peaks when the sample was exchanged for a carefully chosen reference liquid [17]. In order to properly account for effects from spurious higher order modes, the complete transfer function of the cell has been measured and carefully analyzed in a frequency range around a principle resonance frequency. Two cavity resonators have been used. One resonator cell, with fundamental frequency of transducer thickness vibrations $\nu_T=1$ MHz, with cell radius $R_1=35$ mm, and cell length $\ell_r=14$ mm, was suitable at $\nu\leqslant3$ MHz [18]. The other one ($\nu_T=5$ MHz, $R_r=14$ mm, $\ell_r=6$ mm) was designed for measurements at higher frequencies (1.5 MHz$\leqslant\nu\leqslant$15 MHz [19]).

In the range from 3 MHz to 2 GHz α has been also determined by spot frequency measurements. A pulse modulated wave was propagated through a variable path length cell and the attenuation coefficient of the liquid was obtained from the variation of the wave amplitude with cell length. Three specimen cells, each matched to a frequency range, have been employed. These cells mainly differ by their piezoelectric transmitter and receiver unit. Between 3 and 60 MHz, we used disc-shaped quartz transducers ($\nu_T=1$ MHz, $R_T=20$ mm [20]). In measurements from 30 to 500 MHz a cell provided with $LiNbO_3$ transducer discs ($\nu_T=10$ MHz, $R_T=6$ mm [21]) was available. Both cells were operated at the odd overtones $(2n+1)\nu_T$, $n=1,2,\ldots$, of their transducer fundamental frequency ν_T. Above 200 MHz broadband end face excitation of $LiNbO_3$

rods ($R_T = 1.5$ mm, $\ell_T = 10$ mm [22,23]) according to the method by Bömmel and Dransfeld [24] was applied. In measurements below 20 MHz diffraction losses due to the finite transducer diameters had to be taken into account. We used the semiempirical relation

$$U_r(\nu,z) = U_{rmeas}(\nu,z)\exp[-\sqrt{z/(\beta A_r)}]^{g(z)} \qquad (1)$$

to convert the measured receiver voltage values U_{rmeas} into the values U_r to be used in the evaluation routines. In Eq. (1), β is the wave number of the wave propagating in the z direction, and A_r denotes the (circular) transducer surface area and $g(z)$ has been found by calibration measurements with liquids of well-known attenuation coefficient. Possibly existing small instabilities of the apparatus and nonlinearities in the electronic devices have been taken into account by routinely performed calibration procedures in which the cell was replaced by a high precision below cutoff piston attenuator [25] with matched relative attenuation increment [20,21].

C. Sound velocity measurements

In the lower part of the measuring frequency range, the sound velocity c_s of the samples has been derived from successive resonance frequencies ν_{ri}, $i = 1,2, \ldots$, of the cavity cells, also considering the nonequidistant distribution of the ν_{ri} [17,18]. At higher frequencies, the c_s data were obtained from the waviness in the signal transmitted through the cell as resulting from multiple reflections at small transducer spacing.

D. Experimental accuracy

Multiple data recording followed by averaging and digital filtering procedures and a suitable regression analysis lead to negligibly small statistical errors in the α and c_s values. The frequency of measurements was also known and kept constant with an error that was negligibly small. The temperature of the samples was controlled to within ± 0.02 K. Temperature gradients and deviations in the temperature of different cells did not exceed 0.05 K, corresponding with an error of less than 0.1% in the attenuation coefficient of the samples. Care has been taken to avoid variations in the mixture composition during measurements. In order to estimate effects from concentration changes some mixtures have been measured twice. In the second run, the sequence of measurements with the different cells have been passed through in reverse order, using freshly prepared samples. As illustrated by the example in Fig. 2, no changes exceeding the experimental errors in the attenuation coefficient have been found. These errors depend on the particular cell used in a frequency range and also on the attenuation coefficient of the sample liquid itself. Globally, the accuracy of measurements may be characterized as $\Delta\alpha/\alpha = 0.07$, 0.1–3 MHz; $\Delta\alpha/\alpha = 0.025$, 3–30 MHz; $\Delta\alpha/\alpha = 0.01$, 30–500 MHz; $\Delta\alpha/\alpha = 0.015$, 500–2000 MHz; $\Delta c_s/c_s = 0.005$, 0.1–500 MHz; $\Delta c_s/c_s = 0.015$, 500–2000 MHz. Because of the overlaps in the frequency ranges of different apparatus and cells, unnoticed systematic errors exceeding these values appear to be unlikely.

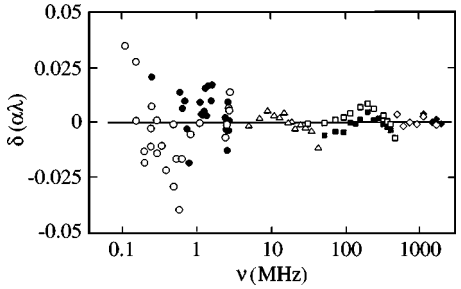

FIG. 2. Deviations $\delta(\alpha\lambda) = \alpha\lambda - R(\nu)$ of the experimental data from the model relaxation spectral function for the mixture of critical composition at 26 °C plotted vs frequency ν. Different symbols indicate different specimen cells, open symbols, first run; closed symbols, second run.

E. Least-squares regression analysis of spectra

It is common practice to discuss ultrasonic attenuation spectra in either format, α/ν^2 versus ν or $\alpha\lambda$ versus ν, where $\lambda = 2\pi/\beta = c_s/\nu$ denotes the wavelength. The former format accentuates the low frequency part of the spectrum and is thus suited to emphasize critical contributions. The latter format stresses high frequency contributions. It is frequently more suitable for the comparison with theoretical models. In order to fit model relaxation spectral functions $R(\nu,P_j)$ to measured $\alpha\lambda$ spectra, we used a Marquardt algorithm [26] to minimize the variance

$$\chi^2 = \frac{1}{N-J-1}\sum_{n=1}^{N}\left(\frac{(\alpha\lambda)_n - R(\nu_n,P_j)}{\Delta(\alpha\lambda)_n}\right)^2. \qquad (2)$$

Here, P_j, $j = 1, \ldots, J$, are the parameters of R and ν_n, $n = 1, \ldots, N$, are the frequencies of measurements. $(\alpha\lambda)_n$ and $\Delta(\alpha\lambda)_n$ denote the attenuation-per-wavelength data and their experimental error, respectively, at ν_n. The use of weighing factors, which are inversely proportional to the absolute errors, in Eq. (2) leads to the same parameter values P_j if the spectra are treated in the frequency normalized format α/ν^2.

III. RESULTS

At two temperatures near the critical one, the frequency normalized ultrasonic attenuation spectra of the *i*-C_4E_1–H_2O mixture of critical composition are shown in Fig. 3. Also displayed in that diagram is the graph of a Debye-type relaxation function

$$\frac{\alpha}{\nu^2} = \frac{A_D'}{1+\omega^2\tau_D^2} + B' \qquad (3)$$

to illustrate that the spectra of the isobutoxyethanol-water mixture are significantly broader than a relaxation term with discrete relaxation time τ_D. In Eq. (3), A_D' denotes the re-

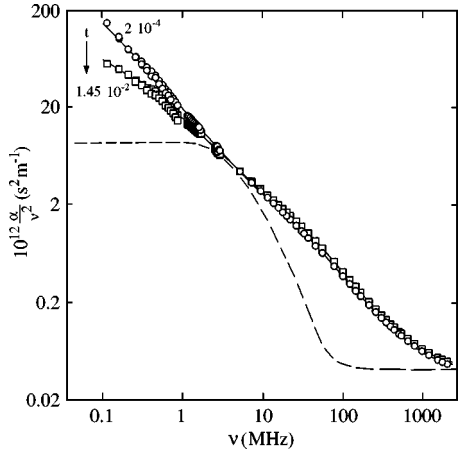

FIG. 3. Frequency normalized ultrasonic attenuation spectra of the i-C_4E_1–water mixture of critical composition at two reduced temperatures t. The dashed curve is the graph of a Debye-type relaxation function [Eq. (3)].

laxation amplitude, B' is an asymptotic high frequency background contribution, and $\omega=2\pi\nu$. At high frequencies, the effect of temperature in our experimental α/ν^2 spectra is small (Fig. 3). At $\nu<2$ MHz, however, frequency normalized attenuation data increase noticeably when the temperature approaches T_c. Hence, at low frequencies, there seems to be a substantial contribution from critical concentration fluctuations. The finding of the concentration fluctuations to contribute in the lower part of our measuring frequency range only points at a small amplitude Γ_0 in the relaxation rate

$$\Gamma(t)=\Gamma_0 t^{-Z_0\tilde{\nu}} \tag{4}$$

of order parameter fluctuations. Here, $t=|T-T_c|/T_c$ is the reduced temperature and Z_0 and $\tilde{\nu}$ are the dynamical critical exponent and the critical exponent of the fluctuation correlation length

$$\xi(t)=\xi_0 t^{-\tilde{\nu}}, \tag{5}$$

with ξ_0 independent of temperature.

In the upper part of the frequency range of measurements, further relaxation mechanisms obviously contribute to the ultrasonic attenuation coefficient of the mixture of critical composition (Fig. 3). This conclusion is substantiated by the spectra for a series of i-C_4E_1–H_2O mixtures of different composition as presented in Fig. 4. In order to accentuate their high frequency characteristics, those data are depicted in the alternative format $\alpha\lambda$ versus ν. Also at compositions substantially different from the critical one, the structure of the spectra doubtlessly evidences the existence of various relaxation mechanisms. A careful analysis of the $\alpha\lambda$ spectra in terms of various relaxation spectral functions, including such representing precritical behavior [27] as well as loss mechanisms associated with thermal and viscoinertial loss mechanisms at particle-suspending medium interfaces [28,29], lead to the conclusion that besides the critical term ("crit") and two Debye terms ("$D1$," "$D2$") also a Hill

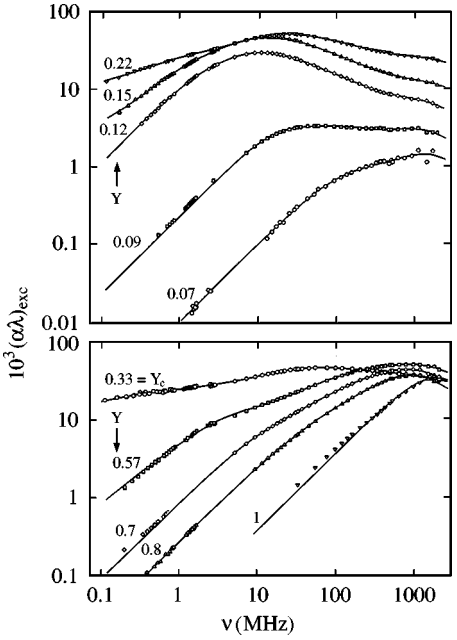

FIG. 4. Ultrasonic attenuation-per-wavelength spectra for i-C_4E_1–water mixtures of different mass fraction Y at 25 °C.

type relaxation term ("H" [30–37]) may contribute to the ultrasonic attenuation. Hence, function

$$R(\nu)=\sum_{i=1}^{2} R_{Di}(\nu)+R_H^{\#}(\nu)+R_{crit}(\nu)+B\nu \tag{6}$$

was used to analytically describe the measured $\alpha\lambda$ spectra at 25 °C. In this function term, $B\nu$ represents the asymptotic high frequency contribution to the sonic attenuation, as according to Refs. [33,34]

$$B=B'c_s=\frac{2\pi^2}{\rho c_s^2}\eta_\ell \tag{7}$$

related to the longitudinal viscosity

$$\eta_\ell=\frac{4}{3}\eta_s+\eta_v, \tag{8}$$

with shear viscosity η_s and volume viscosity η_v. $R_H^{\#}$ denotes the restricted version [32],

$$R_H^{\#}(\nu)=2^{1/s_H-1}A_H^{\#}\frac{\omega\tau_H}{[1+(\omega\tau_H)^{2s_H}]^{3/4s_H}} \tag{9}$$

of the Hill relaxation spectral function [30,31]. In this function, $A_H^{\#}$ is an amplitude, τ_H denotes the principal relaxation time, and s_H is a parameter which controls the width and the shape of the underlying relaxation time distribution function. $R_H^{\#}(\nu)$ has proven suitable for the description of ultrasonic spectra of nonionic surfactant solutions with high critical micelle concentration C [8]. We emphasize that the spectra of the isobutoxyethanol-water mixture cannot be satisfactorily

represented without the restricted Hill term, suggesting micelle formation and decay mechanisms. The Debye terms

$$R_{Di}=\frac{A_{Di}\omega\tau_{Di}}{1+\omega^2\tau_{Di}^2}, \tag{10}$$

follow from Eq. (3) with $A_{Di}=A'_{Di}c_s/(2\pi\tau_{Di})$, $i=1,2$.

The critical term reflecting concentration fluctuations is assumed to be given by the Bhattacharjee-Ferrell ("BF") dynamic scaling theory [35,36]

$$R_{crit}(\nu)=c_sS\nu^{-\delta}I_{BF}(\Omega), \tag{11}$$

with a frequency independent amplitude S and an exponent $\delta=\alpha_0/(Z_0\tilde{\nu})$. Here, $\alpha_0=0.11$ is the specific heat critical exponent [37,38]

$$C_p=\frac{A^+}{\alpha_0}t^{-\alpha_0}(1+D^+t^{\Delta})+E^+t+B^+. \tag{12}$$

Since $\delta=0.06$, the frequency dependence in the $R_{crit}(\nu)$ term is predominantly given by the integral [35] in Eq. (11)

$$I_{BF}(\Omega)=\frac{3}{\pi}\int_0^{\infty}\frac{x^q}{(1+x^2)^2}\frac{K_{BF}(x)}{K_{BF}^2(x)+\Omega^2}dx, \tag{13}$$

with $\Omega=\omega/\Gamma$ denoting the reduced frequency, with $q=3$, and with

$$K_{BF}=x^2(1+x^2)^p, \tag{14}$$

where $p=0.5$. It is only mentioned that besides $p=0.5$ [35,39], $p=1$ has been also used to represent experimental spectra [40].

In the above treatment of concentration fluctuations, the pair distribution function is assumed to follow as

$$g(k)=k^{q-z}C_{OZ}^2(k), \tag{15}$$

from the Ornstein-Zernike (OZ) [41,42] correlation function

$$C_{OZ}(k)=(1+k^2\xi^2)^{-1}, \tag{16}$$

where k denotes a wave vector. If $q=2$ is used in Eq. (15), the pair distribution function as considered in the early Fixman theory of the coupling of critical concentration fluctuations to acoustical fields [43,44] and also in the Kawasaki mode coupling theory of critical sound absorption [45,46] results. Hence, parameter q may be used to relate the scaling function of different theoretical models to one another. Aiming at a reduction of the number of relaxation terms in the analytical representation of the measured spectra, we empirically treated q as an adjustable parameter. However, no satisfactory description of the $\alpha\lambda$ spectra was obtained using $R(\nu)$ with one less noncritical relaxation term and $q\neq 3$.

Following Endo's treatment of noncritical concentration fluctuations [47,48], we have extended the critical term $R_{crit}(\nu)$ assuming a second pathway to exist by which concentration fluctuations may relax parallel to diffusion. If this parallel pathway is a rate process with relaxation rate τ_0^{-1}, $K_{BF}(x)$ is replaced by

$$K(x)=\tau_0^{-1}\xi^2/(2D)+x^2(1+x^2)^p \tag{17}$$

in Eq. (13). Here, D is the mutual diffusion coefficient controlling the diffusive motions. The rate process leads to a shoulder in the critical contribution to the $\alpha\lambda$ spectra [27]. Again, however, a reduction in the number of relaxation terms of the $R(\nu)$ function was not achieved by substituting $K_{BF}(x)$ for $K(x)$.

In order to decrease the expenditure of numerical calculations, the integral $I_{BF}(\Omega)$ in Eq. (11) has been replaced by the simple form [49]

$$I(\Omega)=[1+(\Omega^{\#}/\Omega)^n]^m, \tag{18}$$

with $n=0.5$, $m=-2$, and $\Omega^{\#}=0.1714\Omega_{1/2}$, where $\Omega_{1/2}=2.1$ [36] is the scaled half-attenuation frequency. Taking $\Omega^{\#}=0.821$, $n=0.654$, and $m=-1.87$, the above relation represents the scaling function [49] in the more modern Folk-Moser renormalization group theory of the mode coupling model [50–52]. We also used the latter scaling function which, however, likewise did not allow for a reduction of the number of relaxation terms in the spectral function [Eq. (6)]. We, thus, finally applied the complete spectral function $R(\nu)$ with the Bhattacharjee-Ferrell version

$$I_{BF}(\Omega)=[1+0.414(\Omega_{1/2}/\Omega)^{1/2}]^{-2} \tag{19}$$

of Eq. (18) to the measured spectra of the i-C_4E_1–H_2O mixtures of different composition at 25 °C. The parameters of $R(\nu)$, as following from the nonlinear least-squares regression analysis, are collected in Table II. Because of the large number of adjustable parameters, necessary to represent the measured spectra accordingly, the uncertainty in the parameter values is rather high. Despite of these uncertainties, suggestive trends emerge in the data which will be discussed below. The use of the R_{crit} term in the description of spectra for mixtures of noncritical composition is certainly an empirical approach. Evidently, however, even apart from the critical point, the Bhattacharjee-Ferrell scaling function applies well to the measured spectra. For the noncritical systems, the parameters of this function will not be discussed.

IV. DISCUSSION

A. Relaxation of critical fluctuations

For the mixture of critical composition ultrasonic attenuation spectra have been also recorded as a function of temperature between $T=295.15$ K ($T_c=-4.36$ K, corresponding with $t=0.015$) and $T=299.45$ K ($T_c=-0.06$ K, $t=0.0002$). According to Eq. (11), the Bhattacharjee-Ferrell theory predicts for the sonic attenuation near T_c

$$\alpha/\nu^2=S\nu^{-1.06}+(\alpha/\nu^2)_{bg}, \tag{20}$$

with the background contribution $(\alpha/\nu^2)_{bg}$. Using the low frequency data only (200 kHz$\leqslant\nu\leqslant$2 MHz), the α/ν^2-

TABLE II. Parameters of the relaxation spectral function defined by Eq. (2) used to describe the ultrasonic attenuation spectra of the isobutoxyethanol-water mixtures at 25 °C.

X	A_{BF} (10^{-3}) ±30%	Γ (10^6 s^{-1}) ±50%	A_{D1} (10^{-3}) ±30%	τ_{D1} (ns) 30%	$A_H^{\#}$ (10^3) 30%	τ_H (ns) 30%	s_H 30%	A_{D2} (10^{-3}) 30%	τ_{D2} (ns) 30%	B (ps) 5%
0.011					1	1	0.74	2	0.1	34.0
0.015			3	8	5	2	0.69	4	0.12	34.5
0.020			7	73	59	22	0.67	6	0.11	35.1
0.026	4	0.03	16	95	91	18	0.65	8	0.08	36.6
0.041	21	0.05	12	136	97	12	0.53	13	0.09	39.4
0.061	37	0.08	0.2	109	71	6	0.49	14	0.15	46.2
0.070	39	0.1			68	5	0.48	14	0.15	49.2
0.099	32	0.3	0.5	100	76	2	0.44	19	0.16	56.6
0.168	16	11	7	35	93	1	0.42	34	0.14	64.7
0.262	3	125	3	12	78	1	0.40	44	0.18	81.1
0.379			2	2	42	0.7	0.38	53	0.18	88.6
1.0								62	0.08	73.8

versus-$\nu^{-1.06}$ plot at $t=0.0002$, in fact, defines a straight line (Fig. 5). Hence, the background contribution to the frequency normalized attenuation is largely independent of ν. The slope of the line yields the amplitude factor $S=(3.4\pm0.1)\times10^{-5}$ s$^{-0.94}$ m^{-1}.

Since close to T_c, the experimental data follow the predictions of the Bhattacharjee-Ferrell theory, we have calculated the scaling function from the low frequency attenuation data as

$$F(\Omega)=(\alpha\lambda)_{crit}(\nu,T)/(\alpha\lambda)_{crit}(\nu,T_c), \tag{21}$$

where

$$(\alpha\lambda)_{crit}(\nu,T)=\alpha\lambda(\nu,T)-(\alpha\lambda)_{bg}(\nu,T) \tag{22}$$

is taken as the difference between the measured data and the background part. As $A_{D1}=0$ at $T=T_c$ (Table II), the background part is given by

$$(\alpha\lambda)_{bg}(\nu,T)=R_{D2}(\nu,T)+R_H^{\#}(\nu,T)+B(T)\nu, \tag{23}$$

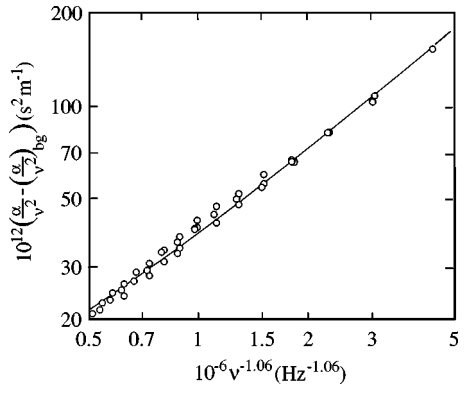

FIG. 5. Frequency normalized attenuation excluding the background part for the i-C_4E_1–water mixture of critical composition at 299.45 K displayed as a function of $\nu^{-1.06}$. The line shows the theoretical prediction for the critical part in the sonic attenuation coefficient [Eq. (20)].

here. Calculating $F(\Omega)$ according to Eq. (21) the relaxation rate Γ of order parameter fluctuations has been used as following from the analytical description of the broadband spectra by the spectral function $R(\nu)$ defined by Eq. (6). In Fig. 6, these Γ values for the mixture of critical composition are displayed as a function of reduced temperature t. As t covers a rather broad range of values, corrections for crossover effects have been applied following the simple procedure proposed by Bhattacharjee and Ferrell [53]. This procedure is based on a crossover correlation factor

$$\tilde{t}/t=[1+\beta/(\xi q_c)]^{1/2}, \tag{24}$$

which relates t to an effective reduced temperature $\tilde{t}$. In Eq. (24), $\beta=1.18$ [53] and the characteristic noncritical crossover wave number q_c has been determined as 0.46×10^{-9} m. At $t=0.0002$ $\tilde{t}/t=1.015$, while at $t=0.015$ $\tilde{t}/t=1.24$. Hence, at larger t noticeable crossover corrections are required which, however, do not alter the qualitative behavior of the relaxation rate data. Using these $\Gamma(t)$ data, the scaling function shown in Fig. 7 follows. It is in reasonable

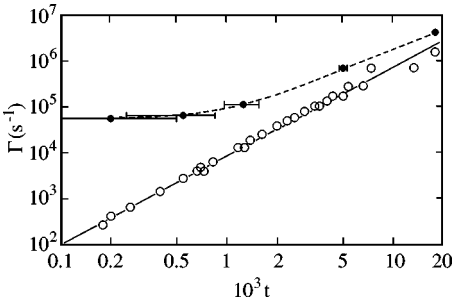

FIG. 6. Relaxation rate Γ of order parameter fluctuations vs reduced temperature t. Points show data from ultrasonic spectrometry after corrections for crossover effects. Error bars indicate an uncertainty of ±0.1 K in the critical temperature. Circles show Γ values from static and dynamic light scattering [60]. The full line is the graph of the power law [Eq. (4)] with the theoretical exponent $Z_0\tilde{\nu}=1.93$.

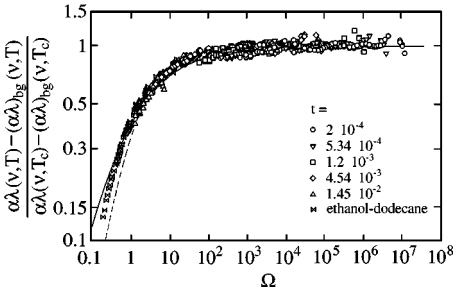

FIG. 7. Scaling function data for the i-C_4E_1–water mixture of critical composition at five reduced temperatures t and for the ethanol-dodecane mixture of critical composition [54]. The full and dashed lines are graphs of the Bhattacharjee-Ferrell [Eq. (19)] and the Folk-Moser [Eq. (18)] scaling function, respectively.

agreement with the scaling function for the simpler system ethanol dodecane [54] and also with the theoretical predictions from the Bhattacharjee-Ferrell and the Folk-Moser theory.

Also shown in Fig. 6 are data of the relaxation rate

$$\Gamma = 2D/\xi^2 \tag{25}$$

of order parameter fluctuations as following from static and dynamic light scattering [10]. These measurements yielded $\xi_0 = (0.316 \pm 0.004)$ nm for the amplitude of the fluctuation correlation length [Eq. (5)] if the exponent in the power law was fixed at $\tilde{\nu} = 0.63$. Additionally,

$$D = D_0 t^{\nu *} \tag{26}$$

was found with $D_0 = (2.66 \pm 0.03) \times 10^{-10}$ m^2 s^{-1} and $\nu^* = 0.643 \pm 0.002$, yielding $\Gamma_0 = 2D_0/\xi_0^2 = 5.3 \times 10^9$ s^{-1}. Hence, as mentioned above, the amplitude in the relaxation rate of the system i-C_4E_1–H_2O is rather small, e.g., $\Gamma_0 = 35 \times 10^9$ s^{-1} for methanol-cyclohexane [55], $\Gamma_0 = 122 \times 10^9$ s^{-1}, 3-methylpentane–nitroethane [56], and $\Gamma_0 = 181 \times 10^9$ s^{-1} n-pentanol-nitroethane [57]. Because of the comparatively small Γ_0 value data at $\Omega < 1$ are missing in the experimental scaling function (Fig. 7). Whereas the Γ data from the static and dynamic light scattering follow Eq. (4) with the universal exponent $Z_0 \tilde{\nu} = 1.93$ (Fig. 6), the relaxation rates from the ultrasonic spectra are noticeably larger and the exponent in the dependence upon the reduced temperature is significantly smaller than $Z_0 \tilde{\nu}$, if there exists power law behavior at all. This result attracts attention since normally the Γ data from ultrasonic spectra either comply with the theoretically predicted power law or exhibit a tendency rather toward amplitudes Γ_0 smaller than those from light scattering, provided the half-attenuation frequency in the scaling function [Eq. (19)] is fixed at $\Omega_{1/2} = 2.1$. We suggest that the special characteristics in the relaxation rates of the isobutoxyethanol-water system are due to the presence of different parallel pathways of relaxation in the relevant time (respectively, frequency) domain. Likely, the formation of oligomeric micellar structures offers such a pathway in addition to the diffusion controlled concentration fluctuations. This line of reasoning includes the idea that the process occuring in parallel to the concentration fluctuations indeed couples to the sonic field but not to the optical field, so that it does not contribute to the relaxation rate Γ determined by light scattering. If this is true, then the ultrasonic spectra strictly should not be analyzed in terms of a linear superposition of common relaxation spectral functions, as the $R(\nu)$ function defined by Eq. (6). Rather a coupling of the concentration fluctuations to a chemical mode, similar to Endo's ansatz [Eq. (17)], should be considered in a rigorous treatment of the spectra.

The Bhattacharjee-Ferrell theory relates to the amplitude of the critical term in the frequency normalized sonic attenuation [Eq. (20)] of the mixture of critical composition

$$S = \frac{\pi^2 \delta C_{pc} c_s(T_c)}{2T_c} \left[\frac{\Omega_{1/2} \Gamma_0}{2\pi} \right]^{\delta} \frac{g^2}{C_{pb}^2} \tag{27}$$

to the adiabatic coupling constant g as well as the singular part C_{pc} and background part C_{pb} of the heat capacity

$$C_p = C_{pc} t^{-\alpha_0} + C_{pb}. \tag{28}$$

Using $C_{pc} = A^+/\alpha_0$ and $C_{pb} = B^+$ [Eq. (12)] and $A^+ = 6.1$ J/kg K as well as $B^+ = 3740$ J/kg K [11], $g = 1.3$ follows from $S = 3.4 \times 10^{-5}$ s$^{-0.94}$ m^{-1} (Fig. 5) and $c_s(T_c) = 1456.97$ m/s. If $X = 0.27$ [37,57,58], and $\rho(T_c) = 0.9715$ g cm^{-3} is used, the two-scale factor universality relation [38]

$$\xi_0 = X \frac{k_B}{A^+ \rho(T_c)} \tag{29}$$

yields $A^+ = 8.9$ J/kg K, resulting in somewhat smaller value $g = 1.1$. Alternatively, the adiabatic coupling constant, according to

$$g = C_p \rho_c \left[\frac{dT_c}{dp} - \frac{T \alpha_p^c}{\rho C_p} \right] \tag{30}$$

may be calculated from the variation dT_c/dp of the critical temperature with pressure along the critical line and the thermal expansion coefficient α_p^c at constant pressure. With $dT_c/dp = (39.8 \pm 0.2) \times 10^{-3}$ K bar^{-1} and $\alpha_p^c = (0.67 \pm 0.02) \times 10^{-3}$ K^{-1} [16] or $\alpha_p^c = (0.8 \pm 0.1) \times 10^{-3}$ K^{-1} [59], $g = 1.3$ follows, in agreement with the value from the ultrasonic measurements. This is another confirmation of the low frequency contribution to the ultrasonic spectra to be correctly assigned to critical fluctuations in the concentration.

B. Micelle kinetics

Let us return to the assumption of a critical micelle concentration for the isobutoxyethanol-water system. In Fig. 8, the amplitudes of the Hill-type relaxation term are displayed along with the aqueous solutions of the cationic surfactant n-heptylammonium chloride (HepACl) and of the nonionic surfactant triethylene glycol monohexyl ether (C_6E_3). For the latter systems, the existence of micellar structures is in-

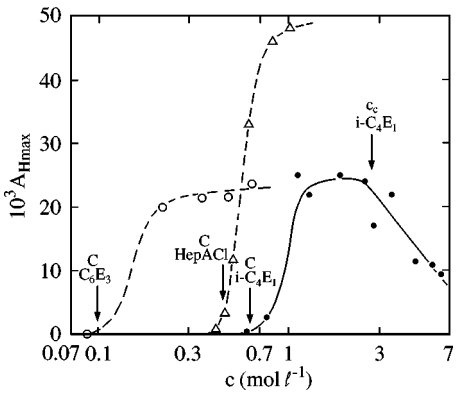

FIG. 8. Maximum amplitude in the Hill relaxation spectral term [Eq. (33)] vs surfactant concentration c for the i-C_4E_1–water mixture at 25 °C (●), for C_6E_3–H_2O mixtures at 17 °C (○, [62]), and for aqueous solutions of the cationic surfactant *n*-heptyl ammonium chloride at 25 °C (Δ,[61]).

disputable, even though the critical micelle concentrations are likewise high: $C=0.4$ mol/ℓ, HepACl, 25 °C [61,62]; $C=0.098$ mol/ℓ, C_6E_3, 17 °C [61]. For reasons of comparison, A_{Hmax} data are shown, because the spectra for the HepACl-H_2O system had been represented by the complete Hill function [30–32]

$$R_H(\nu)=\frac{A_H(\omega\tau_H)^{m_H}}{[1+(\omega\tau_H)^{2s_H}]^{(m_H+n_H)/(2s_H)}}, \tag{31}$$

instead of the restricted version [Eq. (9), $m_H\equiv 1, n_H\equiv 0.5$]. Parameter

$$A_{Hmax}=2R_H(\nu_{Hmax}) \tag{32}$$

considers the effect of the relaxation time distribution parameters m_H, n_H, $s_H\in(0,1)$ in the amplitude A_H and $A_H^{\#}$, respectively [32]:

$$A_{Hmax}=2A_H[(m_H/n_H)^{m_H}(1+m_H/n_H)^{-(m_H+n_H)}]^{1/(2s_H)}. \tag{33}$$

Here, $\nu_{Hmax}=(2\pi\tau_{Hmax})^{-1}$ is the frequency at which the Hill spectral function adopts its maximum value

$$\left.\frac{dR_H(\nu)}{d\nu}\right|_{\nu_{Hmax}}=0, \quad \left.\frac{d^2R_H(\nu)}{d\nu^2}\right|_{\nu_{Hmax}}<0. \tag{34}$$

The relaxation time τ_{Hmax} is related to the characteristic Hill relaxation time τ_H as

$$\tau_{Hmax}=\tau_H(m_H/n_H)^{-1/(2s_H)}. \tag{35}$$

The A_{Hmax} data of the i-C_4E_1-H_2O solutions exhibit all characteristics of the ''four-segment'' model [63] proposed to describe the main aspects of the behavior of short-chain amphiphiles in solution. The data for the C_6E_3 and HepACl solutions display only the first three segments of this model.

At concentrations distinctly smaller than the critical micelle concentration C only monomers exist. As expected intuitively, no Hill-type ultrasonic attenuation is found ($A_{Hmax}=0$). At c only somewhat smaller than C, however, a gentle increase in A_{Hmax} occurs, in contrast to the predictions of the Teubner-Kahlweit theory of the ultrasonic attenuation of solutions of proper micelles [64,65]. This theory is based on the Aniansson-Wall model of micelle formation in solutions with small C. The Aniansson-Wall model proceeds from an isodesmic scheme of coupled reactions [66–68]

$$N_1+N_{i-1}\underset{k_i^r}{\overset{k_i^f}{\rightleftharpoons}}N_i, \quad i=2,3,\ldots, \tag{36}$$

with nearly Gaussian size distribution

$$(k_{i+1}^r\overline{N}_{i+1}-k_i^r\overline{N}_i)/\overline{N}_i=k_m^r/\sigma^2(i-\overline{m}) \tag{37}$$

of aggregates. Here, i denotes the number of amphiphiles per aggregate, k_i^f and k_i^r are the forward and reverse rate constants, respectively, $\overline{m}$ is the mean aggregation number, and σ^2 is the variance of the size distribution. Assuming, in addition, identical reaction volumes $\Delta V=\Delta V_i$, $i=2,3,\ldots$, for all individual steps in the coupled scheme [Eq. (36)], the Teubner-Kahlweit theory yields

$$A_{Hmax}=\frac{\pi(\Delta V)^2}{\kappa_S^{\infty}RT}\overline{N}_1 x\left(1+\frac{\sigma^2}{\overline{m}}x\right)^{-1} \tag{38}$$

and

$$\tau_{Hmax}^{-1}=k_m^r\left(\frac{1}{\sigma^2}+\frac{x}{\overline{m}}\right), \tag{39}$$

with the adiabatic compressibility κ_S^{∞} extrapolated to frequencies well above the relaxation range and with the scaled concentration

$$x=(c/C-1). \tag{40}$$

These relations predict neither the finite amplitude A_{Hmax} in the ultrasonic relaxation term (Fig. 8) nor with c strongly decreasing relaxation rates τ_{Hmax}^{-1} (Fig. 9) at $c<C$. In the third segment, however, at c somewhat larger than C the A_{Hmax} values follow the Teubner-Kahlweit model: they first increase with c and then flatten at higher concentrations. According to relation (38), the amplitude at high surfactant content

$$A_{Hmax}^{\infty}=\lim_{c\to\infty}A_{Hmax}=\frac{\pi(\Delta V)^2}{\kappa_S^{\infty}RT}C \tag{41}$$

is indeed independent of c if $\overline{N}_1=C$ is assumed. From a physical point of view, A_{Hmax} has to decrease with c at high surfactant concentration since the monomer exchange between the micelles and the suspending phase, which is reflected by the Hill relaxation term, will not exist at low water content. Therefore, the decrease in the amplitude values of the i-C_4E_1–H_2O system at $c>2.2$ mol/ℓ is the expected be-

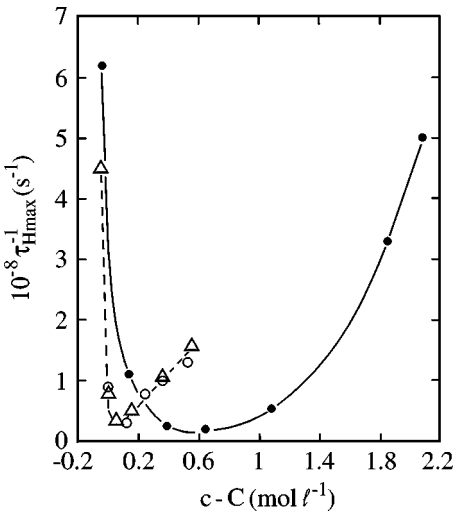

FIG. 9. Relaxation rate τ_{Hmax}^{-1} [Eq. (35)] of the Hill term as a function of surfactant concentration exceeding C for the i-C_4E_1–water mixtures (●, 25 °C), the C_6E_3–H_2O mixtures (○, 17 °C [62]), and the *n*-heptyl ammonium chloride solutions (Δ, 25 °C [61]).

havior. This part of the A_{Hmax}-versus-c relation has been assigned to the fourth segment in the description of short-chain surfactant solutions [63].

In the third segment of the concentration range, the relaxation rate τ_{Hmax}^{-1} of the HepACl and the C_6E_3 solutions follow the Teubner-Kahlweit theory [Eq. (39)]. The τ_{Hmax}^{-1}-versus-c relation for the i-C_4E_1–H_2O system show a broad minimum at $c>C$, probably a reflection of the high critical micelle concentration.

The special characteristics of solutions of short-chain amphiphiles, particularly the finding of $A_{Hmax}\neq 0$ and $d\tau_{Hmax}^{-1}/dc<0$ at $c<C$ and of a relaxation time distribution in the relaxation term representing the monomer exchange, have been qualitatively explained by an extended model of stepwise association [69]. In this model, the size distribution of micellar aggregates is obtained from reasonable assumptions on the forward and reverse rate constants of the coupled reaction scheme [Eq. (36)]. The extended model of micelle kinetics indicates that the relative minimum in the distribution function, located in the oligomer region of aggregation numbers is much less pronounced with short-chain amphiphiles than with surfactants forming proper micelles. Hence, there exists a noticeable concentration of small supramolecular structures in the solutions. In addition, a considerable concentration of oligomeric structures at $c<C$ emerges from the extended model. Furthermore, at concentrations near the critical micelle concentration, the relative maximum in the size distribution of aggregates is missing. Another feature of this extended model of stepwise association is a slight increase in the mean aggregation number $\bar{m}$ with surfactant concentration.

An ultrafast acoustical relaxation process, reflecting the monomer exchange between the oligomeric species and the suspending phase results from the extended model. In conformity with the data shown in Figs. 8 and 9, there exists an ultrasonic relaxation already at concentrations somewhat smaller than C. This relaxation term with unusually high relaxation rate is again due to the formation and decay of small supramolecular premicellar structures. As expected intuitively, the relaxation rate decreases in the concentration range around C when, at increasing c, the aggregation number of these structures increases.

In order to avoid some approximations in the original version of the analytical Teubner-Kahlweit theory, the extended model of stepwise association has been numerically evaluated. That treatment of the coupled reaction scheme [Eq. (36)] revealed a relaxation time distribution in the monomer exchange process, in correspondence with the finding of a restricted Hill relaxation time distribution in our spectra. We thus state that, in fact, the ultrasonic spectra of the i-C_4E_1–H_2O system indicate the formation of micellar structures as characteristic of short-chain surfactant solutions with high critical micelle concentration.

C. Chemical relaxations

In addition to the $R_{crit}(\nu)$ term, the spectra of all mixtures and also of pure i-C_4E_1 display the high frequency Debye term $R_{D2}(\nu)$ with relaxation time τ_{D2} between 0.08 and 0.18 ns (Table II). Except the mixture with the smallest i-C_4E_1 content ($x=0.0113$), the critical mixture ($x=0.0698$), and pure i-C_4E_1 also the low frequency Debye-type relaxation term $R_{D1}(\nu)$ with relaxation time between 2 and 140 ns is found. The spectrum of pure isobutoxyethanol may be alternatively evaluated to yield two Debye relaxations: $A_{D1}=0.0022$, $\tau_{D1}=0.9$ ns; $A_{D2}=0.062$, $\tau_{D2}=0.08$ ns. We mention that somewhat simpler ultrasonic attenuation spectra of aqueous solutions of short-chain 2-ethoxyethanol, 2-isopropoxyethanol, 2-butoxyethanol, and 2-(2-butoxyethoxy)ethanol [70] also contain a high frequency Debye-type relaxation term (0.05 ns$\leqslant\tau_{D2}\leqslant$1 ns). Solutions of both latter systems also display a Debye term at lower frequencies (4 ns$\leqslant\tau_{D1}\leqslant$90 ns) [70].

At least the high frequency Debye term, which doubtlessly exists in the pure organic liquid, obviously reflects a chemical equilibrium of C_iE_j molecules. The formation of hydrogen-bonded dimers

$$2C_iE_j \underset{k^r}{\overset{k^f}{\rightleftharpoons}} (C_iE_j)_2 \tag{42}$$

from monomers, as characteristic for carboxylic acids [71–73], has been considered, as well as structural isomerizations

$$C_iE_j \underset{k^r}{\overset{k^f}{\rightleftharpoons}} (C_iE_j)^*, \tag{43}$$

including the formation of double hydrogen bonded (cyclic, "c") dimers from single H-bonded linear "(ℓ)" ones [71–73]

$$(C_iE_j)_2^{\ell} \underset{k^r}{\overset{k^f}{\rightleftharpoons}} (C_iE_j)_2^{c}. \tag{44}$$

The data for the i-C_4E_1–water mixtures, however, do not follow either concentration dependence

$$\tau_D^{-1} = (8k^f k^r c + k^{r2})^{1/2} \tag{45}$$

or

$$\tau_D^{-1} = k^f + k^r \tag{46}$$

predicted [74] for the dimerization reaction [Eq. (42)] and the structural isomerizations [Eqs. (43) and (44)], respectively. Likely, the inherent concentration dependence in the chemical relaxations is largely masked by the formation of micelles and by the critical fluctuations in concentration of the isobutoxyethanol-water mixtures.

V. CONCLUSIONS

The ultrasonic spectra of isobutoxyethanol-water mixtures reveal the simultaneous formation of micellar structures and of critical concentration fluctuations. Similar results have been obtained recently for various other C_iE_j-water systems for which the existence of a critical micelle concentration is generally accepted [62,75]. The general trends in the ultrasonic spectra of poly(ethylene glycol) monoalkyl ether-water mixtures, including low weight C_iE_j [8] promote the view on the microkinetics of solutions, in which the micelle formation and decay processes and the concentration fluctuations are not considered independently from one another. Rather an idea of a fluctuation controlled monomer exchange between the micelles and the suspending phase seems to fit to the experimental findings. These findings are summarized by the maximum values $(\alpha\lambda)_{max}$ in the ultrasonic attenuation-per-wavelength spectra of C_iE_j-water mixtures, which in Fig. 1 are displayed as a function of the critical micelle concentration. Over a range of more than four orders of magnitude, the $(\alpha\lambda)_{max}$ values are correlated with C of the solutions. Approaching the critical demixing point of the surfactant solutions, diffusion controlled local fluctuations in the micelle distribution are accompanied by local fluctuations in the monomer concentration. Therefore, the monomer exchange between the micelles and the suspending phase is largely governed by the fluctuations in the local concentration of the micelles. Hence, the kinetics of micelle formation and decay which, via volume changes of the monomers, couples to the sonic fields, is subject to concentration fluctuations. In a rigorous model of the ultrasonic attenuation spectra, the micelle formation and decay and the critical concentration fluctuation processes should thus be coupled. The linear superposition of the $R_{crit}(\nu)$ and $R_H^{\#}(\nu)$ relaxation term in our spectral function [Eq. (6)] may thus be considered a simple approximation only.

ACKNOWLEDGMENTS

The authors wish to thank T. Telgmann for many spirited discussions. Also, the financial assistance provided by the Deutsche Forschungsgemeinschaft and the Volkswagen-Stiftung (Hannover, Germany) are gratefully acknowledged.

[1] A.-M. Bellocq, *Critical Behaviour of Surfactant Solutions in Micelles, Membranes, Microemulsions and Monolayers* (Springer, Berlin, 1994).
[2] J.V. Sengers and J.M.H. Levelt Sengers, Annu. Rev. Phys. Chem. **37**, 189 (1986).
[3] M.A. Anisimov, *Critical Phenomena in Liquids and Liquid Crystals* (Gordon and Breach, Philadelphia, 1991).
[4] L.M. Brown, *Renormalization* (Springer, Berlin, 1993).
[5] C. Domb, *The Critical Point: A Historical Introduction to the Modern Theory of Critical Phenomena* (Taylor and Francis, London, 1996).
[6] M.E. Fisher, Rev. Mod. Phys. **70**, 653 (1998).
[7] H.E. Stanley, Rev. Mod. Phys. **71**, 5358 (1999).
[8] T. Telgmann and U. Kaatze, Langmuir **18**, 3068 (2002).
[9] R.J. Fanning and P. Kruus, Can. J. Chem. **48**, 2052 (1970).
[10] S. Limberg, L. Belkoura, and D. Woermann, J. Mol. Liq. **73** and **74**, 223 (1997).
[11] W. Würz, M. Grubic, and D. Woermann, Ber. Bunsenges. Phys. Chem. **96**, 1460 (1992).
[12] S. Nishikawa and T. Yamaguchi, Bull. Chem. Soc. Jpn. **56**, 1585 (1983).
[13] S. Nishikawa and T. Uchida, J. Solution Chem. **12**, 771 (1983).
[14] K.-V. Schubert, R. Strey, and M. Kahlweit, Prog. Colloid Polym. Sci. **84**, 103 (1991).
[15] K.-V. Schubert, R. Strey, and M. Kahlweit, J. Colloid Interface Sci. **141**, 21 (1991).
[16] H.J. Zimmer and D. Woermann, Ber. Bunsenges. Phys. Chem. **95**, 533 (1991).
[17] F. Eggers and U. Kaatze, Meas. Sci. Technol. **7**, 1 (1996).
[18] F. Eggers, U. Kaatze, K.H. Richmann, and T. Telgmann, Meas. Sci. Technol. **5**, 1131 (1994).
[19] U. Kaatze, B. Wehrmann, and R. Pottel, J. Phys. E: Sci. Instrum. **20**, 1035 (1987).
[20] U. Kaatze, V. Kühnel, K. Menzel, and S. Schwerdtfeger, Meas. Sci. Technol. **4**, 1257 (1993).
[21] U. Kaatze, K. Lautscham, and M. Brai, J. Phys. E: Sci. Instrum. **21**, 98 (1988).
[22] U. Kaatze and K. Lautscham, J. Phys. E: Sci. Instrum. **51**, 402 (1988).
[23] U. Kaatze, V. Kühnel, and G. Weiss, Ultrasonics **34**, 21 (1996).
[24] H.E. Bömmel and K. Dransfeld, Phys. Rev. Lett. **1**, 234 (1958).
[25] U. Kaatze and K. Lautscham, J. Phys. E: Sci. Instrum. **19**, 1046 (1986).
[26] D.W. Marquardt, J. Soc. Ind. Appl. Math. **2**, 2 (1963).
[27] A. Rupprecht and U. Kaatze, J. Phys. Chem. A **103**, 6485 (1999).
[28] U. Kaatze, C. Trachimow, R. Pottel, and M. Brai, Ann. Phys. **5**, 13 (1996).
[29] T. Stieler, F.-D. Scholle, A. Weiss, M. Ballauf, and U. Kaatze, Langmuir **17**, 1743 (2001).
[30] R.M. Hill, Nature (London) **275**, 96 (1978).

[31] R.M. Hill, Phys. Status Solidi B **103**, 319 (1981).
[32] K. Menzel, A. Rupprecht, and U. Kaatze, J. Acoust. Soc. Am. **104**, 2741 (1998).
[33] G. Herzfeld and T. Litovitz, *Absorption and Dispersion of Ultrasonic Waves* (Academic, New York, 1959).
[34] U. Kaatze, T.O. Hushcha, and F. Eggers, J. Solution Chem. **29**, 299 (2000).
[35] A.C. Flewelling, R.J. DeFonseka, N. Khaleeli, J. Partee, and D.T. Jacobs, J. Chem. Phys. **104**, 8048 (1996).
[36] P.F. Rebillot and D.T. Jacobs, J. Chem. Phys. **109**, 4009 (1998).
[37] J.K. Bhattacharjee and R.A. Ferrell, Phys. Rev. A **24**, 1643 (1981).
[38] R.A. Ferrell and J.K. Bhattacharjee, Phys. Rev. A **31**, 1788 (1985).
[39] H. Dunker, D. Woermann, and J.K. Bhattacharjee, Ber. Bunsenges. Phys. Chem. **87**, 591 (1983).
[40] H. Tanaka and Y. Wada, Phys. Rev. A **32**, 512 (1985).
[41] L.S. Ornstein and F. Zernike, Phys. Z. **19**, 134 (1918).
[42] L.S. Ornstein and F. Zernike, Phys. Z. **27**, 762 (1926).
[43] M. Fixman, J. Chem. Phys. **33**, 1363 (1960).
[44] M. Fixman, Adv. Chem. Phys. **4**, 175 (1964).
[45] K. Kawasaki, Phys. Rev. **120**, 291 (1966).
[46] K. Kawasaki, Ann. Phys. (N.Y.) **61**, 1 (1970).
[47] H. Endo, J. Chem. Phys. **92**, 1986 (1990).
[48] H. Endo and K. Honda, J. Chem. Phys. **115**, 7575 (2001).
[49] T. Telgmann, R. Behrends, and U. Kaatze, J. Chem. Phys. **117**, 9828 (2002).
[50] R. Folk and G. Moser, Europhys. Lett. **41**, 177 (1998).
[51] R. Folk and G. Moser, Phys. Rev. E **57**, 683,705 (1998).
[52] R. Folk and G. Moser, Phys. Rev. E **58**, 6246 (1998).
[53] J.K. Bhattacharjee and R.A. Ferrell, Physica A **250**, 83 (1998).
[54] S.Z. Mirzaev, T. Telgmann, and U. Kaatze, Phys. Rev. E **61**, 542 (2000).
[55] S.Z. Mirzaev, Dissertation, Uzbekistan Academy of Sciences, Tashkent, 1996.
[56] C.W. Garland and G. Sanchez, J. Chem. Phys. **79**, 3090 (1983).
[57] T. Hornowski and M. Labowski, Acta Phys. Pol. A **79**, 671 (1991).
[58] E.A. Clerke, J.V. Sengers, R.A. Ferrell, and J.K. Bhattacharjee, Phys. Rev. A **27**, 2140 (1983).
[59] C. Bervellier and C. Godrèche, Phys. Rev. B **21**, 5427 (1980).
[60] F. Höhn, Dissertation, Universität zu Köln, Köln, 1992.
[61] T. Telgmann and U. Kaatze, J. Phys. Chem. B **101**, 7758 (1997).
[62] T. Telgmann and U. Kaatze, J. Phys. Chem. A **104**, 1085 (2000).
[63] T. Telgmann, Dissertation, Georg-August-Universität, Göttingen, 1997.
[64] M. Teubner, J. Phys. Chem. **83**, 2917 (1979).
[65] M. Kahlweit and M. Teubner, Adv. Colloid Interface Sci. **13**, 1 (1980).
[66] E.A.G. Aniansson and S.N. Wall, J. Phys. Chem. **78**, 1024 (1974).
[67] E.A.G. Aniansson and S.N. Wall, J. Phys. Chem. **79**, 857 (1975).
[68] E.A.G. Aniansson, Prog. Colloid Polym. Sci. **70**, 2 (1985).
[69] T. Telgmann and U. Kaatze, J. Phys. Chem. B **101**, 7766 (1997).
[70] K. Menzel, A. Rupprecht, and U. Kaatze, J. Phys. Chem. B **101**, 1255 (1997).
[71] R.D. Corsaro and G. Atkinson, J. Chem. Phys. **55**, 1971 (1971).
[72] D. Tabuchi, Mem. Inst. Sci. Ind. Res., Osaka Univ. **28**, 67 (1971).
[73] A. Rupprecht, H. Krah, V. Kühnel, and U. Kaatze, in *Proceedings of the World Congress on Ultrasonics*, edited by J. Herbertz (GEFAU, Duisburg, 1995), p. 511.
[74] H. Strehlow, *Rapid Reactions in Solution* (VCH, Weinheim, 1992).
[75] T. Telgmann and U. Kaatze, J. Phys. Chem. A **104**, 4846 (2000).